Journal of Optimization in Industrial Engineering Vol.12, Issue 1, Winter and Spring 2019, 133- 149
DOI: 10.22094/JOIE.2018.764.1487

Multi-Response Optimization of Grooved Circular Tubes Filled With Polyurethane Foam as Energy Absorber

Shima Shahravi [a], Mohammad Javad Rezvani [b,*], Ali Jahan[b]

[a] *M.Sc, Semnan Branch, Islamic Azad University, Semnan, Iran*

[b] *Energy and Sustainable Development Research Center, Semnan Branch, Islamic Azad University, Semnan, Iran.*

Received 05 May 2017; Revised 06 May 2018; Accepted 06 June 2018

Abstract

The main objective of this research is to improve the design and performance of the polyurethane foam-filled thin-walled aluminum grooved circular tubes using multi-response optimization (MRO) technique. The tubes are shaped with the inner and the outer circular grooves at different positions along the axis. For this aim, several numerical simulations using ABAQUS finite element explicit code are performed to study the energy absorption of these structures. The effects of the grooves distance, tube diameter, grooves depth, foam density, and tube thickness are investigated on the crash worthiness parameters of grooved circular tubes. Finite-element analysis is performed along the lines defined by design of experiments (DOE) technique at different combinations of the design parameters. The MRO is carried out using the mathematical models obtained from response surface methodology (RSM) for two crashworthiness parameters termed as the specific energy absorption (SEA) and the crushing force efficiency (CFE). Finally, by analyzing all the design criteria including the absorbed energy of tube, the mass of tube, the mean crushing load, and the maximum crushing load, the optimal density of polyurethane foam and geometric parameters were obtained through both multi-objective optimization process and Pareto diagram. A comparison of the obtained results indicates the significance of grooves distance and the inner diameter of the tube as the most influential parameters.

Keywords: Grooved tubes; Crush force efficiency; Specific energy absorption; Multi-response optimization; Design of experiments

1. Introduction

Thin-walled tubes with different shapes have several applications in transportation systems such as cars, trains, cruise ships, and also elevator where they are used as energy absorbents to dissipate energy in the collision events and vehicle accidents. Energy absorbents systems are used to protect automotive and its occupants from the effects of sudden impacts that occurs during collisions. Such structures are designed with a low weight to promote public safety. In crashworthiness applications, global bending must be avoided since it can cause a significant reduction in the energy absorption capacity. To improve energy absorption, collapse mode, and stability of the shock absorbers, thin-walled tubes are filled with a lightweight material. Foams are a new class of materials with extremely low densities and unique combination of excellent mechanical that help the stability of the tubes and improve the energy absorption. Many studies were experimentally performed using foams under both quasi-static and dynamic axial crushing load conditions (Seitz berger et al., 2000; Yamada, Banno, Xie, & Wen, 2005). A comprehensive experimental study was carried out on the thin-walled columns filled with aluminum foam by A. Hanssen & Langseth, 1996; A. Hanssen, Langseth, & Hopperstad, 1999. They investigated the crushing behavior of the foam-filled aluminum square tubes under quasi-static axial loading. They reported significant increases of crushing force via direct compressive strength of the foam and from the interaction between the foam and wall column. An experimental study was carried out to investigate of the axial deformation behavior of triggered circular aluminum extrusions filled with aluminum foam under both quasi-static and dynamic loading conditions by A. G. Hanssen, Langseth, & Hopperstad, 2000. The behavior of foam-filled thin-walled tubes with different cross-sectional shapes under axial compression was investigated by Thornton Thornton, 1980. The results indicated that mean crushing load of the foam-filled tube was more than that of the individual tube and the foam in total due to the interaction effects of both components. Reid et al. Reid, Reddy, & Gray, 1986, studied effect of filling thin-walled circular metal tubes with low-density polyurethane foam under both quasi-static and dynamic axial loading. They found that the stability of crushing improved by using polyurethane foam. Therefore, the crushing load will increase either due to the crush resistance of the foam or because of its influence on changing the buckling mode of the tube wall from diamond or mixed mode to ring mode. So far, several methods have been presented to reduce initial peak load and enhancement of crush force efficiency; e.g., creating circumferential grooves from the outer and inner surfaces of the tube (Damghani Nouri & Rezvani, 2012; Eyvazian, K. Habibi, Hamouda, & Hedayati, 2014; Niknejad, Abedi, Liaghat, & Zamani

*Corresponding author Email address: m.rezvani@semnaniau.ac.ir

Nejad, 2012; M. Rezvani, M. D. Nouri, & H. Rahmani, 2012; Rezvani & Nouri, 2013). It has been evidenced that the grooves reduce the overall wave amplitude and the mean collapse load, a property that is favorable in an efficient energy absorption device. Furthermore, the load-deflection and energy absorption response of grooved tubes could be controlled by changing the distances of circumferential grooves cut alternately inside and outside the tubes. A number of works have been conducted on the subject matter of thin-walled tubes optimization. Zarei & Kröger, 2006,an optimization of cylindrical tubes was performed to maximize the absorbed energy and specific energy absorption. Marzbanrad & Ebrahimi, 2011; Mirzaei, Shakeri, Sadighi, & Seyedi, 2011; Shakeri, Mirzaeifar, & Salehghaffari, 2007,presented multi-objective optimization of thin-walled cylindrical tubes under axial impact with length-to-diameter and diameter-to-thickness ratios as design parameters. Optimization of ringed tube such as rings' number, depth, and width, as well as wall thickness was performed by Salehghaffari, Rais-Rohani, & Najafi, 2011as design parameters while specific energy absorption and maximum crushing load were taken as design objectives.

Considering a high number of design variables for a cylindrical fender and wide range of variations in these variables, finding the optimum conditions using one-factor-at-a-time experiments will be very costly and time-consuming. Using design of experiments (DOE) techniques, particularly response surface methodology (RSM), one will probably be able to consider multiple variables at a time with the lowest number of experiments to reasonably analyze experimental data via statistical analysis and, ultimately, to mathematically model the objectives based on the design parameters(Bahraminasab et al., 2014; Jahan, Ismail, & Noorossana, 2010).

Based on the mentioned literature, making corrugations on thin-walled cylindrical tubes may effectively contribute to crashworthiness characteristics. Therefore, this research is seeking to find the optimum foam density, tube and corrugation dimensions (including tube diameter, corrugation spacing, corrugation depth), and tube thickness at corrugation through multi-response optimization (MRO).

2. Evaluation criteria for energy absorption systems

Desired criteria considered when assessing crashworthiness and structure's safety enhancement are obtained from the load-displacement curve.

2.1 Absorbed energy

The total energy absorbed, $E_{absorbed}$, is equal to the area under the load-displacement curve, where:

Where P and $\delta$are the crush force and crush distance, respectively.

2.2 Mean crushing load

the mean crushing load (P_m) – as one of the most important parameters affecting tubes' behavior under axial load – is equal to the ratio of total absorbed energy to total crushing distance.

2.3 Maximum crushing load

According to Fig. 1, the maximum crushing load (P_{max}) contributes to creating the first fold (which dictates the maximum compressive strength). The ideal energy absorber would attain a maximum load immediately and maintain it for the entire length of the component. In summary, the design goals for an efficient energy absorption device are to have a mean load equivalent to the peak load.

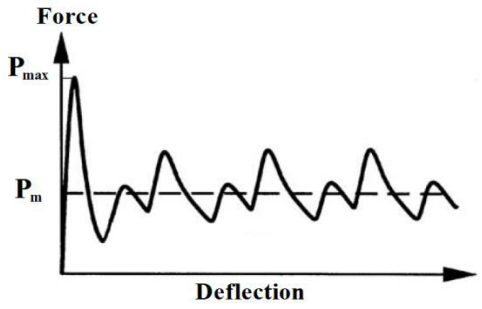

Fig. 1Typical load–displacement curve

2.4 Crushing force efficiency (CFE)

This parameter is used to compare theefficiency of different energy absorbents. It is equal to the ratio of mean crushing load to the maximum crushing load.

2.5 Specific energy absorption (SEA)

SEA provides a way of comparing energy absorption capacity of structures with different masses. This criterion is calculated by the ratio of total absorbed energy to the tube mass:

Where m is total mass of the specimen/structure undergoes deformation. In this research, the SEA and CFE were considered as design objectives among the evaluation criteria. These attributes were selected such that they could properly represent crashworthiness characteristic of the tube while being dependent on other attributes as shown in Eqs.(1), (2), (3),and (4).

3. Materials and Methods

Fig. 2 shows geometric detail parameters of the polyurethane foam-filled grooved circular tube. The grooves are created inside and outside alternately and with the equal distances from the internal and external surfaces of the tubes. As shown in the figure, D_i is the inner diameter of the tube, t is the tube wall thickness, t' is the wall thickness in the groove, W is the groove width, d is the groove depth, and λ is the distance between the grooves.

Design variables and their ranges were selected based on careful studying of literature. The stages of this study are presented in Fig.3. The steps consist of determining the design objectives, creating the DOE, simulation, and validation, creating a mathematical model, and finally optimization.

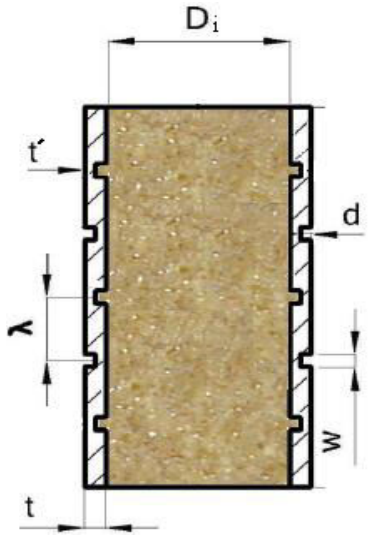

Fig. 2. Details of the design parameters

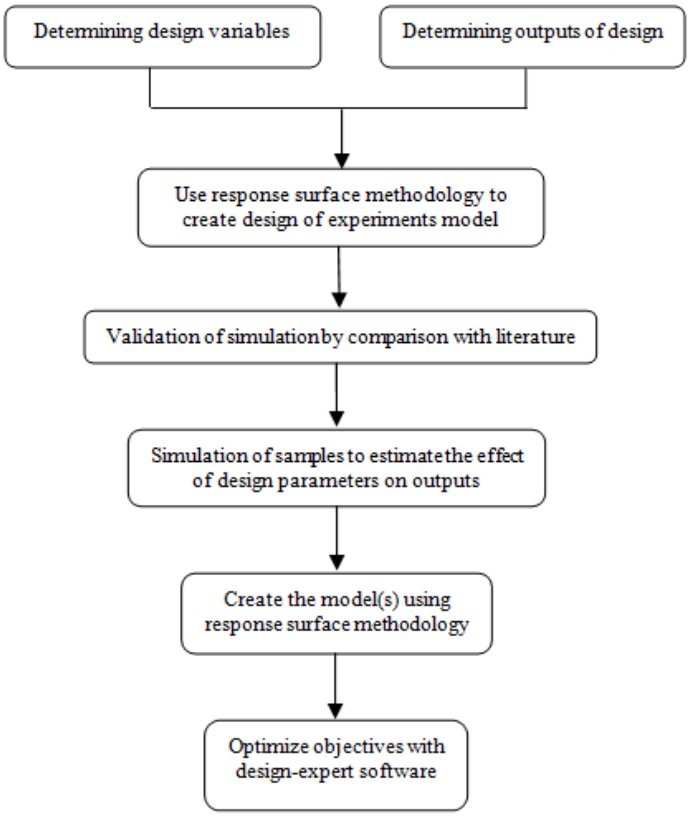

Fig. 3. The used steps for computational experiments in multi-objective design optimization

In this study, the parameters that remain constant (the design constants) include the groove shape (G), the groove length (L), and the groove width (W), which are presented in Table 1.

Table 1
Design constants

Design constants	Unit	Amounts
L	*mm*	200
W	*mm*	4
Groove shape	-	Circular

Also, the ranges of the design variables are as follows:

$$0.6 \leq t' (mm) \leq 1.7 \quad (5)$$

$$0.4 \leq d\ (mm) \leq 1.3 \quad (6)$$

$$60 \leq \rho\ (kg/m^3) \leq 300 \quad (7)$$

$$5 \leq \lambda\ (mm) \leq 16 \quad (8)$$

$$42 \leq D_i (mm) \leq 92 \quad (9)$$

Hosseini Pour and Daneshi2004, demonstrated that creating grooves can reduce the force fluctuations during deformation and improve the uniformity of force-displacement curve and energy absorption criteria. Thus, the variation range of grooves distance (λ) is selected from the grooves distances in the mentioned study by investigating the deformation modes and grooves distances. Many studies have been conducted to evaluate the effect of changing the foam density (ρ) on energy absorption criterion. The range of the variation for this parameter was selected based on the variation of ρ/ρ_s, where ρ is the density of the foam and ρ_s is the density of the solid from which the foam is obtained. The ρ_s value for Polyurethane foam is equal to 1200 kg/m^3(Ashby & Medalist, 1983)

The depth of grooves (d) and the thickness of tube in grooves are related by $t'=t-d$), where $t$is the tube thickness and d is the groove depth. In this study, the changes in the thickness are achieved by varying d and t'. The range of variation in d and $t'$is defined based on the range of the tube thickness. The groove width is selected to be 4 because, as described by S. Hosseinipour & G. Daneshi, 2004, the relation$W \geq \pi d$with groove depth must be satisfied. To evaluate the crashworthiness characteristics, specific energy absorption (SEA) and crushing force efficiency (CFE) were selected as design goals.

3.1. Material properties

3.1.1. Grooved circular tube

Aluminum and magnesium alloys, high strength steels, and composites are all alternatives to soft steel in the thin-walled tubes, especially in the automotive industry. Therefore, series 6061-T6 aluminum alloy was selected for grooved circular tubes. The properties of this material are provided in Table 2 and their stress-strain curve is plotted in Fig. 4 based on the ASTM B557M tensile test (M. Rezvani et al., 2012).

Table 2
Mechanical properties of the alloy Aluminium 6061-T6

Poisson ratio	-	0.33
Density	(kg/m^3)	2700
Young's modulus	(GPa)	69
yield strength	(MPa)	311
Ultimate strength	(MPa)	348

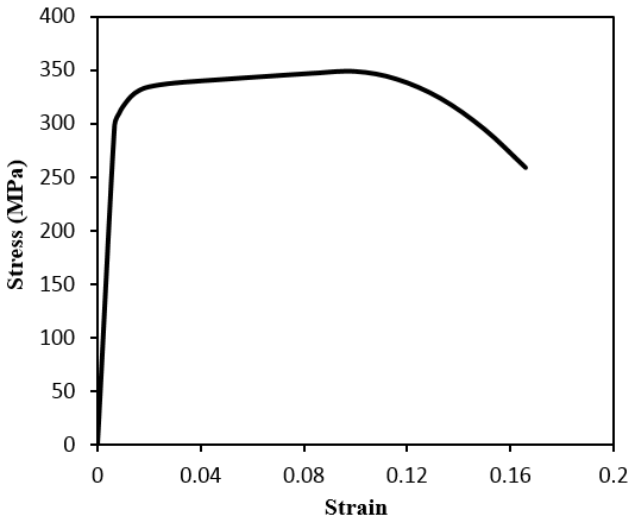

Fig. 4. Stress-strain curve for 6061-T6 Aluminum (M. Rezvani et al., 2012)

3.1.2. Polyurethane foam

Cellular materials, generally known as structural foams, play an important role in many passive safety applications. Energy-absorbing polymeric foams are widely used in the automotive industry to prevent injuries to the occupants in the event of front or side collisions. The use of foamed materials results in a significant improvement in the passive safety of the vehicle, owing to their excellent energy dissipation properties. In addition, they have low apparent density, involve low costs, and allow great design flexibility, as they can be easily modeled in complex geometric parts.

Generally, the stress-strain curves of polymeric foams contain three distinct regions: linear elastic region, plateau region, and densification region. At small strains, usually <5%, the behavior is linearly elastic, with a slope equal to Young's modulus of the foam. Therefore, in the linear elastic region, deformation is controlled by cell walls bending or stretching. This region is followed by a plastic collapse region that is proceeded by spreading the local deformation and collapse to the non-deformed region of the sample. This region is characterized by a loading plateau with either a constant value or slight increase in displacement. In densification region, cell walls start to touch each other and the sample is densified. Avalle, Belingardi, & Montanini, 2001, examined mechanical characteristics of three polymeric foams namely a polypropylene foam, a polyurethane foam, and a polyamide foam. They used the efficiency diagram method to obtain synthetic diagrams useful to characterize the material and to help the design of energy-absorbing components. The results showed that the polypropylene and the polyamide foams exhibited similar properties and were strongly sensitive to strain-rate although their cell structure is different. Also, they found that the polyurethane foams have a completely different behavior with a large intermediate plateau phase and very low sensitivity to the strain-rate. Therefore, in this study, polyurethane foam was used as filler in the circular grooved tube.

The mechanical properties of the existing foam in the design of experiment model are required for simulation. The mechanical properties of these foams are obtained using graphs and tables included in Ashby & Medalist, 1983 and relations of the Gipson model expressed in Eqs. (10) to (13) (Avalle, Belingardi, & Ibba, 2007).

Linear elastic region

$$\sigma = E\varepsilon \quad if \quad \sigma \le \sigma_{yield} \tag{10}$$

Plateau region

$$\sigma = \sigma_{yield} \text{ if } \varepsilon_{yield} \le \varepsilon \le \varepsilon_D(1\text{-}D^{-1/m}) \tag{11}$$

Densification region:

$$\sigma = \sigma_{yield}\frac{1}{D}\left(\frac{\varepsilon_D}{\varepsilon_D\text{-}\varepsilon}\right)^m \text{if} \varepsilon > \varepsilon_D(1\text{-}D^{-1/m}) \tag{12}$$

Where:

$$\varepsilon_D = 1 - 1.4\frac{\rho}{\rho_s} \tag{13}$$

whereσandε are the engineering stress and strain, respectively. E is Young's modulus,$\sigma_{yield}$is the yield strength,$\varepsilon_D$is the densification strain,and m and D are computed based on the deformation micro mechanics of the cell. Parameter D and m are considered density-independent. Gibson suggests the values D=2.73 and m=1.07 for the polyurethane foams (Avalle et al., 2007). Also, the elastic and plastic properties of the different foams are provided in Table 3.

Table 3
Properties of the used foams in the design of experiments model

Density(kg/m^3)	Elastic specification		Plastic specification	
	Young's modulus(MPa)	Poisson ratio	k	ν_p
60	1.6	0	1	0
129.55	16	0	1	0
180	25	0	1	0
230.45	48	0	1	0
300	70	0	1	0

3.2. Experimental Design Model

The response surface method as a subgroup of the methods for DOE is a useful tool for the development, improvement, and optimization of the designs and processes. Table 4 shows the computational experimental design. The values of the design variables in the process f DOE are 43experimental modes that have been obtained by Design-Expert of t ware Vaughn, 2007based on based on central composite design (Table 5). The DOE consists of 32factorial points, a central point, and 10 axial points that were determined based o n define d ranges.

Table 4
Computational experimental design

Row	Factor 1	Factor 2	Factor 3	Factor 4	Factor 5
Factors	A:Thickness of tube in groove *mm*	B:Depth of grooves *mm*	C:Density of foam kg/m^3	D:Distance of grooves *mm*	E:Internal diameter of tube *mm*
1	0.92	0.66	129.55	8.19	56.49
2	1.38	0.66	129.55	8.19	56.49
3	0.92	1.04	129.55	8.19	56.49
4	1.38	1.04	129.55	8.19	56.49
5	0.92	0.66	230.45	8.19	56.49
6	1.38	0.66	230.45	8.19	56.49
7	0.92	1.04	230.45	8.19	56.49
8	1.38	1.04	230.45	8.19	56.49
9	0.92	0.66	129.55	12.81	56.49
10	1.38	0.66	129.55	12.81	56.49
11	0.92	1.04	129.55	12.81	56.49
12	1.38	1.04	129.55	12.81	56.49
13	0.92	0.66	230.45	12.81	56.49
14	1.38	0.66	230.45	12.81	56.49
15	0.92	1.04	230.45	12.81	56.49
16	1.38	1.04	230.45	12.81	56.49
17	0.92	0.66	129.55	8.19	77.51
18	1.38	0.66	129.55	8.19	77.51
19	0.92	1.04	129.55	8.19	77.51
20	1.38	1.04	129.55	8.19	77.51
21	0.92	0.66	230.45	8.19	77.51
22	1.38	0.66	230.45	8.19	77.51
23	0.92	1.04	230.45	8.19	77.51
24	1.38	1.04	230.45	8.19	77.51
25	0.92	0.66	129.55	12.81	77.51
26	1.38	0.66	129.55	12.81	77.51
27	0.92	1.04	129.55	12.81	77.51
28	1.38	1.04	129.55	12.81	77.51
29	0.92	0.66	230.45	12.81	77.51
30	1.38	0.66	230.45	12.81	77.51
31	0.92	1.04	230.45	12.81	77.51
32	1.38	1.04	230.45	12.81	77.51
33	0.6	0.85	180	10.5	67
34	1.7	0.85	180	10.5	67
35	1.15	0.4	180	10.5	67
36	1.15	1.3	180	10.5	67
37	1.15	0.85	60	10.5	67
38	1.15	0.85	300	10.5	67
39	1.15	0.85	180	5	67
40	1.15	0.85	180	16	67
41	1.15	0.85	180	10.5	42
42	1.15	0.85	180	10.5	92
43	1.15	0.85	180	10.5	67

Table 5
Coded and un-coded values for central composite design

Coded design points	Un-coded values				
	A:Thickness of tube in groove	B:Depth of grooves	C:Density of foam	D:Distance of grooves	E:Internal diameter of tube
-2.37841	0.6	0.4	60	5	42
-1	0.92	0.66	129.55	8.19	56.49
0	1.15	0.85	180	10.5	67
1	1.38	1.04	230.45	12.81	77.51
2.37841	1.7	1.3	300	16	92

3.3. Finite element modeling of grooved cylindrical tubes

In this study, the non-linear finite element platform ABAQUS 5.6 was used for the numerical analysis of the crushing behavior of the foam-filled grooved circular tubes. In order to verify the numerical simulations, a specimen consisting 17 grooves was simulated based on the given geometry (Table 6) that extracted from reference M. J. Rezvani, M. D. Nouri, & H. Rahmani, 2012. As can be seen from Fig. 5, a good conformity exists between experimental and numerical simulation tests. Therefore, the numerical simulation is able to estimate the crashworthiness parameters in circular grooved tubes.

Table 6
Specification of the used experimental reference specimen for validation of the simulation model (M. J. Rezvani et al., 2012)

Geometrical dimensions of tube	Unit	Amounts
Length	*mm*	117.6
Thickness	*mm*	2
External diameter	*mm*	47.5
Internal diameter	*mm*	43.5
Groove width	*mm*	3
Groove depth	*mm*	1
Distance of grooves	*mm*	6.7
Number of grooves	-	17
Groove shape	-	Circular

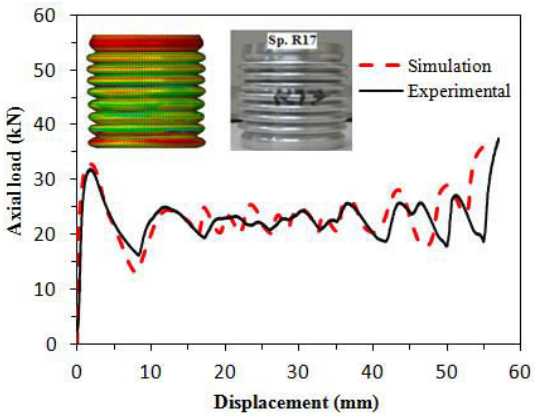

Fig. 5. Comparison of the experimental test and numerical simulation of the load-displacement curve for a circular 17 grooves with reference (M. J. Rezvani et al., 2012)

The explicit dynamic analysis is used for simulation of the circular grooved tubes. Aluminum tube and polyurethane foam are modeled by C3D8R 8-nodes brick elements with nonlinear asymmetric deformations. According to Fig. 6, the rigid body is used for modeling the upper and lower plates describing the universal machine jaws in the quasi-static analysis.

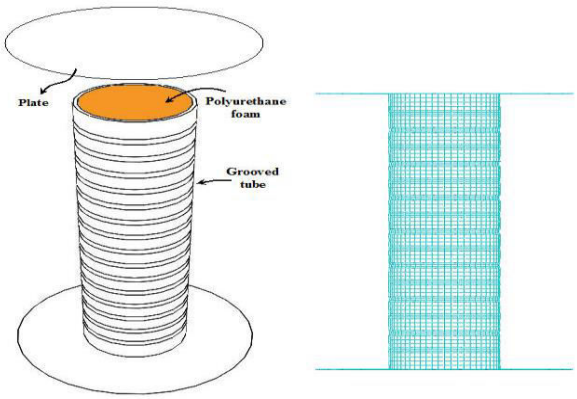

Fig. 6. a) Loading and boundary condition arrangement on grooved circular tube; b) Finite element mesh

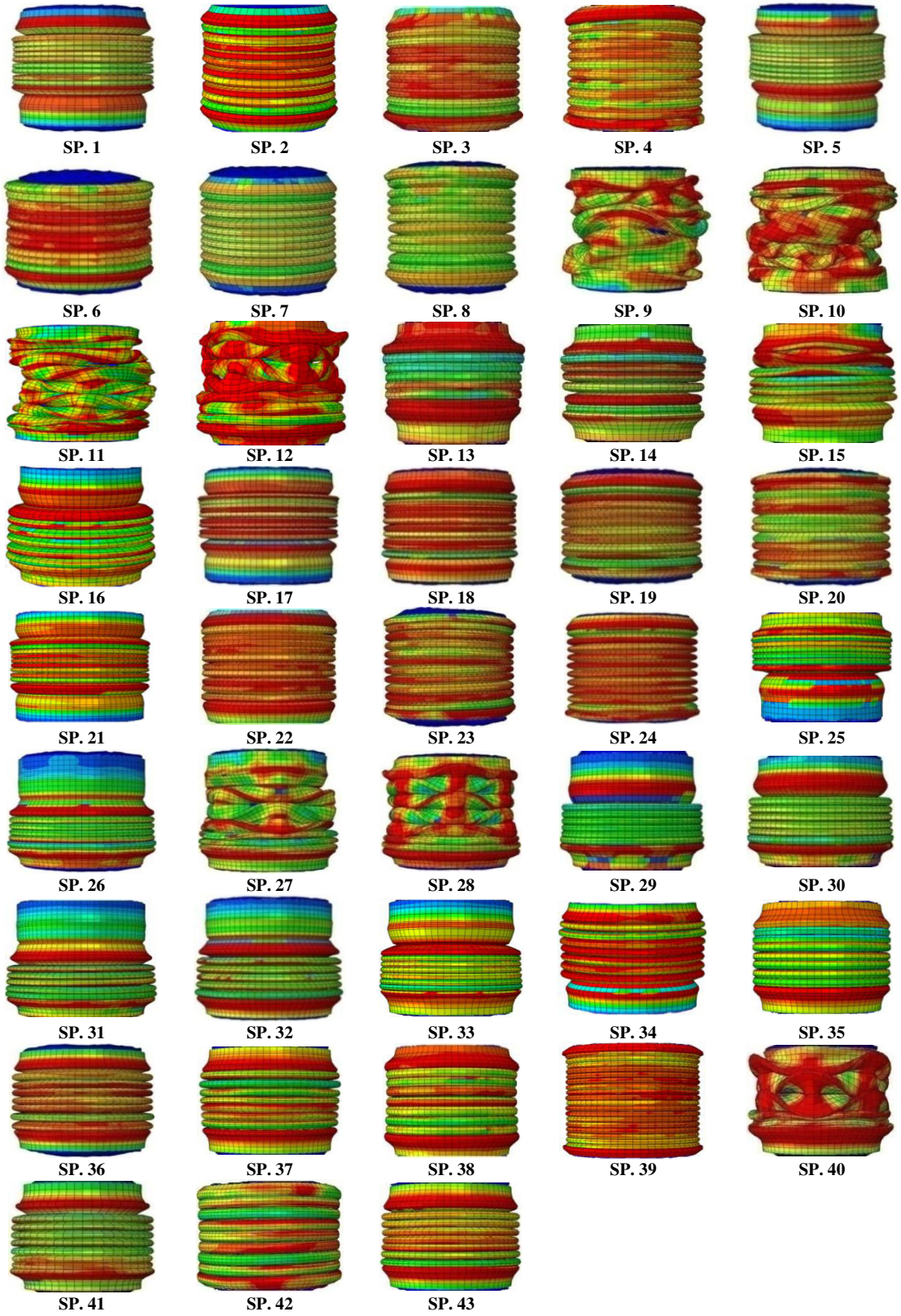

Fig. 7. Crushing mode of the samples

Based on Fig.7, the final deformation of the samples (11,10,9,and 40) is asymmetric. By comparing the samples, it is identified that increasing distance between the grooves, the reduction of the foam density, small thickness, and diameter of the tube lead to a symmetric crushing mode. The deformation of samples (12, 15, 27,and28) is a combination of symmetric and a symmetric folds. The crushing mode is improved to some extent in the sample s with higher density, higher thickness, and diameter of the tube and changes to a combined mode of

symmetric and a symmetric folds. Accordingly, one can state that the a symmetric deformation of the samples with the short distance between the grooves and low foam density can be improved by increasing the tube diameter and thickness. Besides, the symmetric collapse occurs in the samples with the short distance between the grooves (higher number of the grooves) and higher foam density. The effect of the grooves on improving the collapse of thin-walled cylindrical tubes is also supported by results of similar works Daneshi & Hosseinipour, 2002; Hosseinipour & Daneshi, 2003; S. J. Hosseinipour & G. H. Daneshi, 2004; Niknejad et al., 2012; M. J. Rezvani et al., 2012.

The load-displacement curve is shown for some design samples in Figs.8and9. As can be seen in the figures, when the crushing force is maximum the material is yielded at the end of the tube and the force is severely reduced by creating the first plastic hinge. This force declination continues until a fold is formed completely. Then, the next hinge takes form and again reduces and increases in the force can be observed. So, it can be said that each peak in the load-displacement curve represents the formation of a fold. However, in case of a low number of grooves (more distance between the grooves), a series of instability can be seen in the curve, which providesmore stable conditions compared to a case of a large number of grooves (lower distance between the grooves). As a result, less fluctuation is observed in the load-displacement curve. Although the presence of grooves in the tube decreases the energy absorption, it creates uniform plastic hinges during the crushing. Energy absorption criterion and other criteria consisting of crush force efficiency, mean and maximum crushing loads were calculated based on the relations applied to define the design goal and considering the values obtained from simulation (Table 7).As can be seen, a decrease in the grooves' distance leads to a corresponding increase in the crush force efficiency and a decrease in the specific energy absorption. Also, the results show that samples with a higher foam density have a higher crushing force efficiency compared to the empty ones.

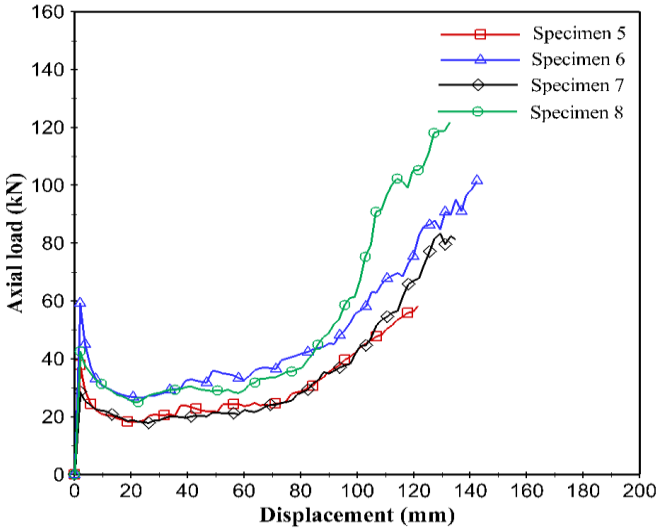

Fig. 8. Load-displacement curves for the samples 5-8

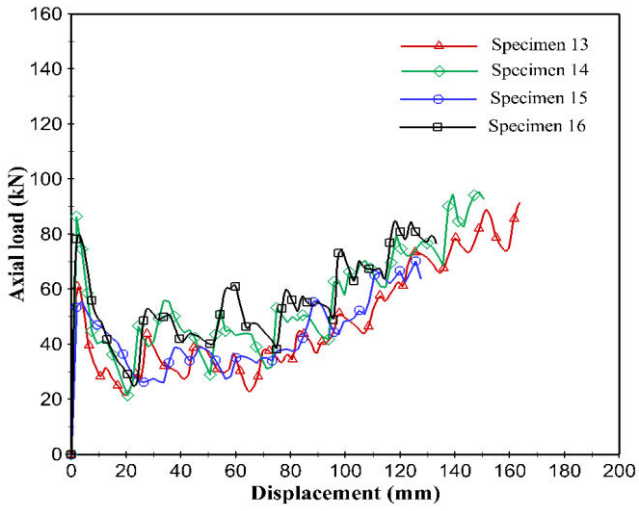

Fig. 9 Load-displacement curves for the samples 13-16

Table 7
Simulation results of the samples

Sample	$m_{tube}\ (kg)$	$P_{max}\ (kN)$	$P_{mean}\ (kN)$	$E_{absorbed}\ (kJ)$	$CFE(\%)$	$SEA(kJ/kg)$
1	0.203	37.386	17.963	1.449	48.046	7.147
2	0.250	57.829	26.331	2.123	45.531	8.507
3	0.229	28.116	16.426	1.322	58.423	5.783
4	0.276	42.271	24.626	1.985	58.258	7.192
5	0.253	38.027	22.822	1.837	60.015	7.255
6	0.300	59.227	33.283	2.681	56.196	8.936
7	0.279	28.627	21.407	1.727	74.781	6.186
8	0.327	42.735	30.338	2.442	70.992	7.478
9	0.218	61.547	31.759	2.568	51.602	11.769
10	0.267	91.042	44.038	3.549	48.372	13.289
11	0.250	54.113	32.714	2.636	60.455	10.534
12	0.300	82.290	42.196	3.402	51.277	11.352
13	0.270	60.922	32.930	2.658	54.054	9.840
14	0.319	86.423	43.203	3.485	49.990	10.923
15	0.302	43.487	36.305	2.936	64.621	9.584
16	0.352	78.177	47.146	3.797	60.307	10.779
17	0.310	41.857	23.287	1.878	55.633	6.052
18	0.374	67.335	35.013	2.821	51.998	7.553
19	0.345	28.682	20.872	1.682	72.772	4.871
20	0.409	47.651	31.533	2.544	66.176	6.219
21	0.406	43.102	31.944	2.575	74.112	6.350
22	0.469	68.540	44.860	3.615	65.452	7.710
23	0.441	29.518	29.907	2.411	101.320	5.474
24	0.504	47.938	41.005	3.308	85.537	6.558
25	0.333	72.468	31.655	2.553	43.682	7.671
26	0.399	102.641	42.435	3.424	41.344	8.588
27	0.376	66.000	35.158	2.835	53.269	7.537
28	0.443	93.833	46.065	3.719	49.092	8.403
29	0.431	64.534	39.218	3.163	60.771	7.335
30	0.498	103.064	51.531	4.154	49.999	8.340
31	0.475	67.608	43.892	3.540	64.922	7.447
32	0.542	94.979	56.168	4.526	59.138	8.351
33	0.263	36.683	22.375	1.807	60.996	6.871
34	0.390	92.973	47.686	3.842	51.290	9.843
35	0.286	46.407	32.252	2.606	69.498	9.100
36	0.365	51.216	36.792	2.964	71.838	8.122
37	0.244	57.426	23.831	1.926	41.499	7.890
38	0.408	62.988	44.757	3.608	71.056	8.850
39	0.318	24.274	26.649	2.189	109.786	6.884
40	0.339	82.583	48.576	3.922	58.821	11.578
41	0.177	50.805	28.565	2.308	56.224	13.009
42	0.508	63.937	40.015	3.230	62.585	6.362
43	0.326	61.292	33.273	2.680	54.285	8.215

4.2. Results of statistical analysis

The effect of the design variables on specific energy absorption, crushing for c efficiency, and relevant optimum values were estimated using Design-Expert software. Analysis of variance (ANOVA) was done to study the importance of the variables and their interaction effects. In the model analysis, the sum of squares (SS) and the mean squares (MS) were calculated by evaluating the responses. In addition, in this analysis, there are two parameters named F-Value and P-value. F-Value represents the ratio of the MS to MS error, and P-Value states the importance of a factor. P-Value=1 and P-Value=0 correspond to the least and most important factors, respectively. Typically, in the RSM model, terms with P-Value<0.05 can be used to predict the response behavior, so they are preserved in the mathematical model.

4.2.1Specific energy absorption index

Table8shows ANOVA results for the specific energy absorption. Regarding that P-Value in the modelis less than0.05, it can be concluded that the model is statistically

valid. By Investigating the P-Value for model parameters, it can be concluded that the main effective variables are grooves distance, the inner diameter of the tube, tube thickness in the grooves, and the grooves depth, respectively. Moreover, the interaction effects of two factors such as foam density-grooves distance and grooves distance-inner diameter of the tube are remarkable. The interaction effects of two factors means that the effect of one factor on the response changes is dependent on the level of the other factor.

Table 8
ANOVA results for specific energy absorption in the grooved cylindrical tubes

Source	Sum of Squares	df	Mean Square	F Value	P-Value
Model	156.50	15	10.43	24.35	<0.0001
A-Thickness of tube (t')	15.94	1	15.94	37.19	<0.0001*
B-Depth of grooves (d)	5.69	1	5.69	13.28	0.0011*
C-Density of foam (ρ)	0.052	1	0.052	0.12	0.7306
D-Distance of grooves (λ)	66.77	1	66.77	155.83	<0.0001*
E-Internal diameter of tube (D_i)	53.29	1	53.29	124.37	<0.0001*
AB	0.085	1	0.085	0.20	0.6597
AC	2.332e-003	1	2.332e-003	5.442e-003	0.9417
AD	0.26	1	0.26	0.60	0.4453
AE	0.048	1	0.048	0.11	0.7412
BC	0.50	1	0.50	1.16	0.2909
BD	1.17	1	1.17	2.73	0.1099
BE	0.48	1	0.48	1.11	0.3016
CD	2.55	1	2.55	5.95	0.0216*
CE	0.82	1	0.82	1.91	0.1778
DE	8.86	1	8.86	20.68	0.0001*
Residual	11.57	27	0.43		
Cor Total	168.07	42			

* Denotes significant factors

Due to the interaction effects of the parameters, they are fitted to the second-order model to predict the specific energy absorption (Eq.(14)). The amount of R-Square is equal to 0.84, which means that only 84% of the variation in the SEA is predictable by the design factors (t', d,λ, and D_i).

$$SEA = -2.82952 + 6.57974 \times t' - 11.60821 \times d + 2.24386 \times \lambda + 0.03361 \times D_i - 2.4187 \times 10^{-3} \times \rho \times \lambda - 0.021648 \times \lambda \times D_i \quad (14)$$

By normalizing Eq.(14), we have:

$$SEA = 8.32 + 0.61 \times t' - 0.36 \times d + 1.24 \times \lambda - 1.11 \times D_i - 0.28 \times \rho \times \lambda - 0.53 \times \lambda \times D_i \quad (15)$$

Eq. (15) shows the importance of each design variable on the specific energy absorption. The effects of changing the tube thickness in the groove, groove depth, grooves number, and the inner diameter of the tube on the specific energy absorption are shown in Fig. 10. As shown in this figure, increasing the thickness of tube in the grooves leads to a corresponding increase in the specific energy absorption. Moreover, increasing the groove depth, the grooves number (reduction of grooves distance), and the inner diameter of tube leads to a decrease in specific energy absorption. Both Fig. 10and Eq. (15) reveal that the effects of grooves distance and the inner diameter of the tube on the specific energy absorption are higher than those of other parameters.

The interaction effects of grooves distance-foam density and the grooves distance-inner diameter of the tube are presented in the Fig. 11. Fig. 11(a) shows the 3D surface interaction effect while keeping other design variables constant. According to Fig. 11(b), by increasing distance of grooves (decreasing the number of grooves), the specific energy absorption is increased, but the level increase is higher for the tubes with less internal diameter.

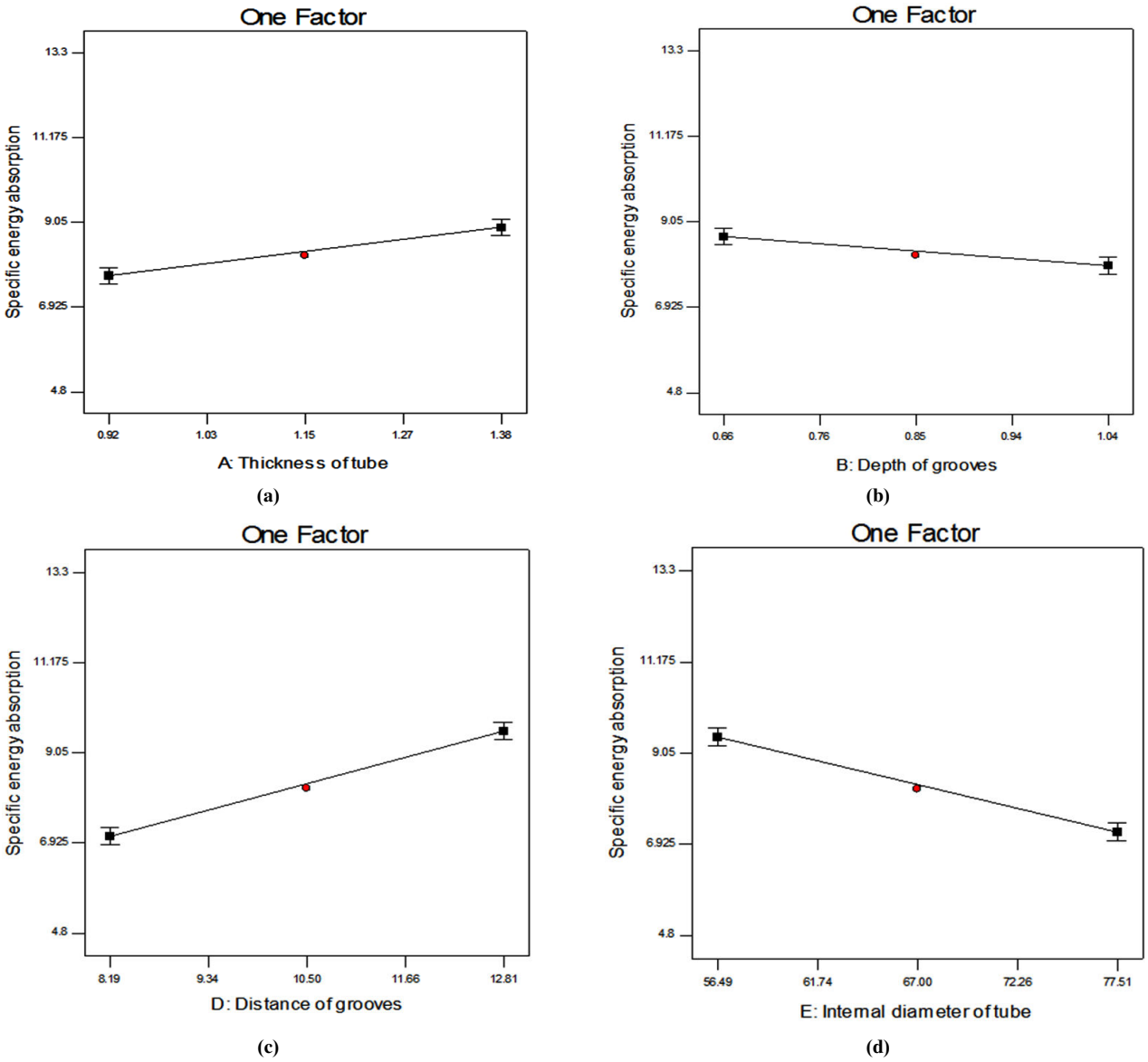

Fig. 10. The effects of design variables on the specific energy absorption:
(a) Tube thickness in grooves, (b) Foam density, (c) Grooves distance , (d) Inner diameter of tube

4.2.2 Crushing force efficiency index

Table 9 shows the ANOVA results for the crushing force efficiency index. It is seen that important factors are foam density, grooves distance, groove depth, and the thickness of tube in grooves, respectively.

Table 9
ANOVA results for the crushing force efficiency in the grooved circular tubes

Source	Sum of Squares	df	Mean Square	F Value	P-Value
Model	5396.74	5	1079.35	12.12	<0.0001
A-Thickness of tube (t')	394.81	1	394.81	4.43	0.0421*
B-Depth of grooves (d)	1107.00	1	1107.00	12.43	0.0011*
C-Density of foam (ρ)	1881.04	1	1881.04	21.11	<0.0001*
D-Distance of grooves (λ)	1871.39	1	1871.39	21.01	<0.0001*
E-Internal diameter of tube (D_i)	142.51	1	142.51	1.60	0.2139
Residual	3296.22	37	89.09		
Cor Total	8692.97	42			

* Denotes significant factors

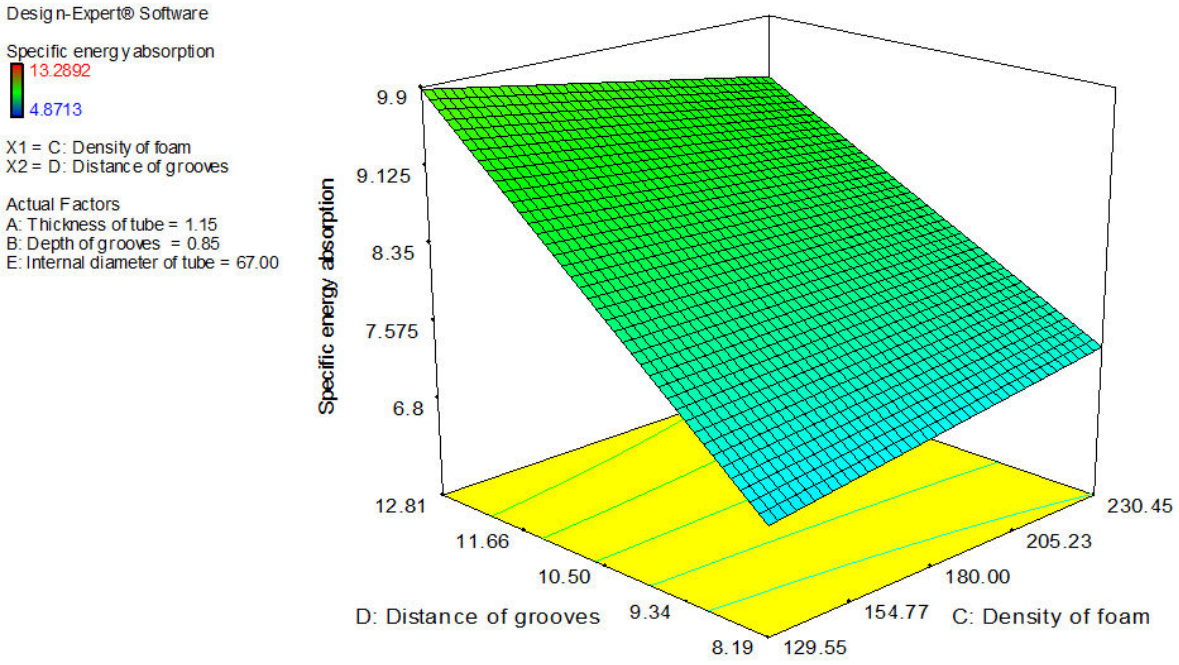

(a)

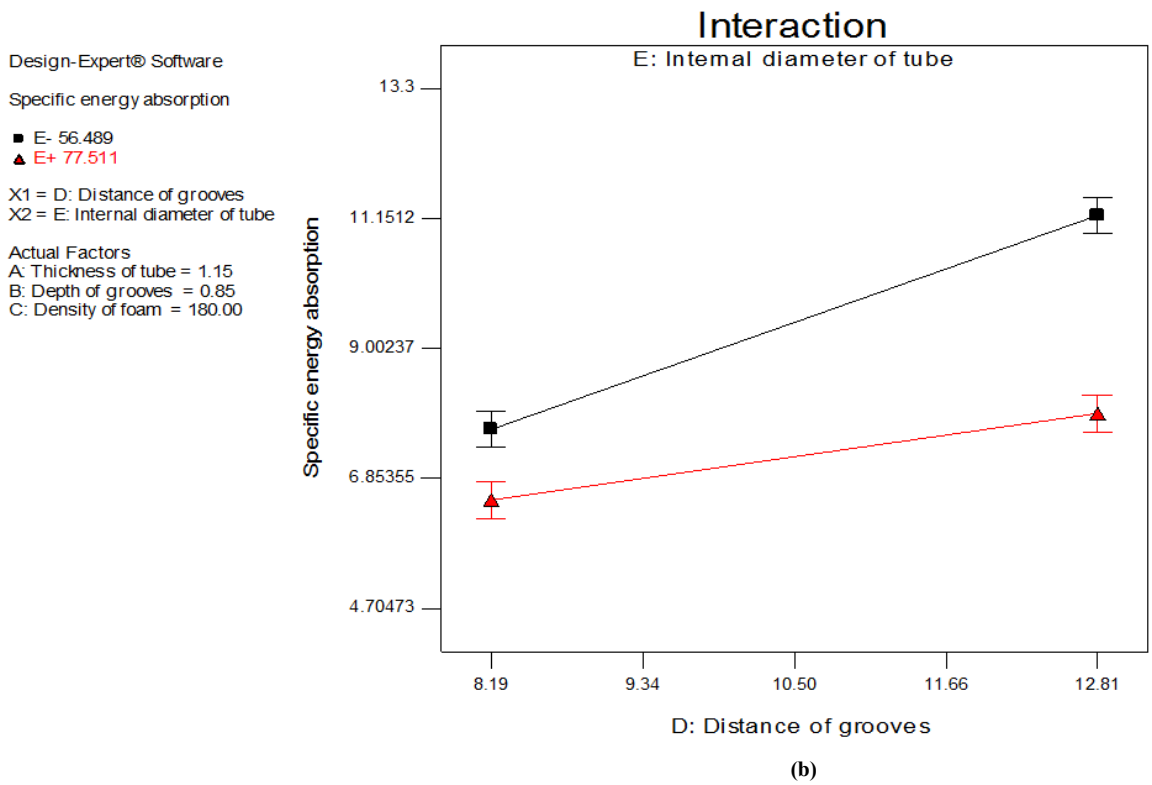

(b)

Fig. 11. The interaction effects on specific energy absorption:
(a) Grooves distance and the foam density, (b) Grooves distance and the inner diameter of the tube

The variation in the crush force efficiency is predicted based on the linear model presented in Eq. (16).The amount of R-Square is equal to 0.62, which means that 62% of the variation in the CFE can be predicted by the regression model.

$$CFE = 48.35190 - 13.05585 \times t' + 26.71994 \times d + 0.13061 \times \rho - 2.84246 \times \lambda \quad (16)$$

By normalizing Eq. (16), we have:

$$CFE = 61.28 - 3.02 \times t' + 5.06 \times d + 6.59 \times \rho - 6.57 \times \lambda \quad (17)$$

Eq. (17) shows the effect of each design variable on the crush force efficiency. It is seen that an increase in groove depth and the foam density leads to the increase in the crush force efficiency and the increase in thickness of the grooves. Besides, grooves distance leads to a drop in the crush force efficiency. It is noteworthy that the effect of the foam density and the grooves distance on the crush force efficiency is higher than that of other parameters.

4-3 Multi-objective optimization

In this research, a multi-objective optimization was carried out using Design-Expert software to find the optimal values of the design variables. The aim is to maximize the specific energy absorption and the crushing force efficiency simultaneously. The objective functions and the design variables for this modeling are shown in Eqs. (18-26).

$$Max\ f_1(x_1, x_2, \dots) = Max\ SEA\ (t', d, \rho, \lambda, D_i) \quad (18)$$

$$Max\ f_2(x_1, x_2, \dots) = Max\ CFE\ (t', d, \rho, \lambda, D_i) \quad (19)$$

$$f_1 = SEA\ (t', d, \rho, \lambda, D_i) = -2.82952 + 6.57974 \times t' - 11.60821 \times d + 2.24386 \times \lambda + 0.03361 \times D_i - 2.4187 \times 10^{-3} \times \rho \times \lambda - 0.021648 \times \lambda \times D_i \quad (20)$$

$$f_2 = CFE\ (t', d, \rho, \lambda, D_i) = 48.35190 - 13.05585 \times t' + 26.71994 \times d + 0.13061 \times \rho - 2.84246 \times \lambda \quad (21)$$

$$0.6 \leq t' (mm) \leq 1.7 \quad (22)$$

$$0.4 \leq d\ (mm) \leq 1.3 \quad (23)$$

$$60 \leq \rho\ (kg/m^3) \leq 300 \quad (24)$$

$$5 \leq \lambda\ (mm) \leq 16 \quad (25)$$

$$42 \leq D_i (mm) \leq 92 \quad (26)$$

Considering the same importance for objective functions, optimal values and the related responses are shown in Table10. Clearly, by changing the importance level of objectives, the optimum point might change.

Table 10
The optimum values for design variables

Design variables					SEA (*kJ/kg*)	CFE (%)
t' (mm)	d (mm)	ρ (kg/m^3)	λ (mm)	D_i (mm)		
0.92	1.04	230.45	12.66	56.49	9.93956	67.9977

Results of the optimal sample have been compared with those of the numerical simulation in Table11. Moreover, the load-displacement curve and the crushing load of the optimal design are shown in Fig. 12. As the results show, the optimal design has a symmetrical collapse and the crashworthiness parameters obtained through the simulation have an acceptable conformity with the optimization results through mathematical modeling. Therefore, the stable collapse can be made of the absorbent by designing a foam-filled grooved circular tube based on the design parameters presented in Table 10.

Table 11
Comparing the obtained crashworthiness parameters with simulation and optimization

Crashworthiness parameters	Simulation	Optimization
$m_{tube}\ (kg)$	0.3	-
$P_{max}\ (kN)$	62.378	-
$P_{mean}\ (kN)$	38.032	-
$E_{absorbed}\ (kJ)$	3.705	-
CFE (%)	60.970	67.998
$SEA\ (kJ/kg)$	12.350	9.939

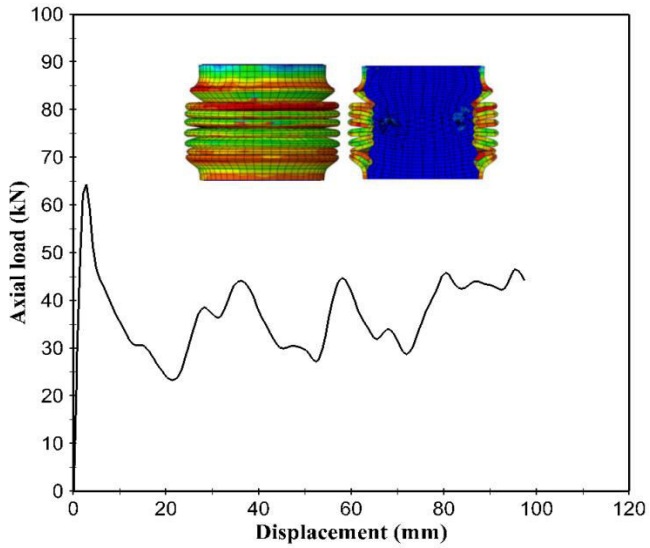

Fig. 12. The force-displacement diagram for the optimum design

The results of a multi-objective optimization problem usually consist of a group of optimal solutions known as the Pareto front. None of the solutions could be superior to the other solutions unless the designer preferences are defined. In Fig. 13, a set of points for 43 designs of experiments are shown in the areas of the objectives. Pareto optimal responses were identified by the plus sign (+) in the areas of the objectives. As mentioned earlier, the main purpose of this article is to maximize two functions SEA and CFE or minimize 1/SEA and 1/CFE. According to Fig. 13, the design indicated by an arrow (multiplication sign (×)) is more desirable than both other Pareto optimal solutions and the optimum point obtained from the multi-objective optimization process; probably due to the low R-squared index of the regression models (Sections 4-2-1 and 4-2-2). This is the sample 15 in the design scenarios listed in Table 7.

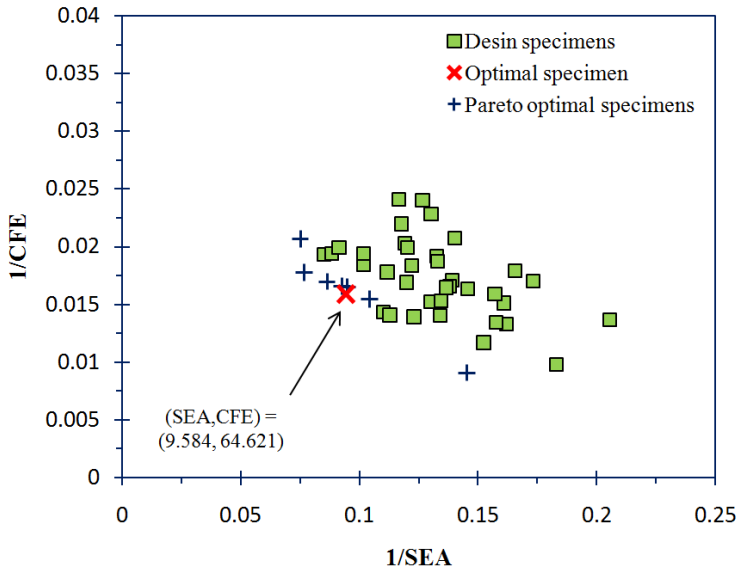

Fig. 13. A set of optimum points in Pareto chart

5. Conclusion

From viewpoint of the thin-walled circular tubes design, influence of design parameters on the objectives discovered through multi-objective optimization process. It was revealed that the increasing the number of grooves and the foam density led to improve the collapse mode of the circular tubes. Also, the load fluctuations in load-displacement curve reduced by increasing the number of grooves. In this study, the effect of design variables including the tube thickness in groove, the groove distance, the groove depth, the internal diameter of tube and the density of polyurethane foam were estimated on the response of specific energy absorption and crush force efficiency. It was found that the SEA can non-linearly be

predicated by foam density, tube diameter, grooves distance, and tube thickness of the groove. Increasing in internal diameter of tube will result in reducing the SEA. Whereas, the foam density, distance between grooves and tube thickness in the grooves will have positive effect on SEA. The CFE was related to the grooves distance, foam density, groove depth, tube diameter, and tube thickness of the grooves by a linearly model. By Increasing the distance between grooves and tube thickness in the grooves, the CFE decreased. On the other hand, the CFE increased by increasing the foam density, internal diameter of tube and groove depth.

In terms of multi-objective optimization, a systematic combined RSM-FEA-MCDM approach was developed and exemplified for a better description of the method. It was shown that although ANOVA and the consecutive regression models clearly reveal the influence of the design variables on the objectives, usually due to a low R-squared index, some deficiencies exist in explaining the variations of objectives by the design variables. In such cases, the Pareto diagram can be helpful for the designer in order to find the best solutions among the available design alternatives. However, the application of Pareto diagram is limited to only two design objectives and there is a need for other MODM tools such goal programming or even MADM techniques. Further research could usefully explore optimum design conditions in the presence of more performance objectives as well as economic and environmental aims. Also, other types of sections such as conical, hexagonal, square, or rectangular could be included in future multi objective design optimization research.

References

Ashby, M. F., & Medalist, R. M. (1983). The mechanical properties of cellular solids. *Metallurgical Transactions A, 14*(9), 1755-1769.

Avalle, M., Belingardi, G., & Ibba, A. (2007). Mechanical models of cellular solids: parameters identification from experimental tests. *International Journal of Impact Engineering, 34*(1), 3-27.

Avalle, M., Belingardi, G., & Montanini, R. (2001). Characterization of polymeric structural foams under compressive impact loading by means of energy-absorption diagram. *International Journal of Impact Engineering, 25*(5), 455-472.

Bahraminasab, M., Sahari, B. B., Edwards, K. L., Farahmand, F., Hong, T. S., Arumugam, M., & Jahan, A. (2014). Multi-objective design optimization of functionally graded material for the femoral component of a total knee replacement. *Materials & Design, 53*, 159-173.

Damghani Nouri, M., & Rezvani, M. J. (2012). Experimental Investigation of Polymeric Foam and Grooves Effects on Crashworthiness Characteristics of Thin-Walled Conical Tubes. *Experimental Techniques*, no-no. doi:10.1111/j.1747-1567.2012.00825.x

Daneshi, G. H., & Hosseinipour, S. J. (2002). Grooves effect on crashworthiness characteristics of thin-walled tubes under axial compression. *Materials & design, 23*(7), 611-617.

Eyvazian, A., K. Habibi, M., Hamouda, A. M., & Hedayati, R. (2014). Axial crushing behavior and energy absorption efficiency of corrugated tubes. *Materials & Design, 54*, 1028-1038. doi:10.1016/j.matdes.2013.09.031

Hanssen, A., & Langseth, M. (1996). *Development in aluminium based crash absorption components.* Paper presented at the Norwegian–French Industrial Conference, Paris.

Hanssen, A., Langseth, M., & Hopperstad, O. (1999). Static crushing of square aluminium extrusions with aluminium foam filler. *International Journal of Mechanical Sciences, 41*(8), 967-993.

Hanssen, A. G., Langseth, M., & Hopperstad, O. S. (2000). Static and dynamic crushing of circular aluminium extrusions with aluminium foam filler. *International Journal of Impact Engineering, 24*(5), 475-507.

Hosseinipour, S., & Daneshi, G. (2004). Experimental studies on thin-walled grooved tubes under axial compression. *Experimental mechanics, 44*(1), 101-108.

Hosseinipour, S. J., & Daneshi, G. H. (2003). Energy absorbtion and mean crushing load of thin-walled grooved tubes under axial compression. *Thin-Walled Structures, 41*(1), 31-46. doi:10.1016/s0263-8231(02)00099-x

Hosseinipour, S. J., & Daneshi, G. H. (2004). Experimental studies on thin-walled grooved tubes under axial compression. *Experimental mechanics, 44*(1), 101-108.

Jahan, A., Ismail, M. Y., & Noorossana, R. (2010). Multi response optimization in design of experiments considering capability index in bounded objectives method. *Journal of Scientific & Industrial Research, 69*, 11-16.

Marzbanrad, J., & Ebrahimi, M. R. (2011). Multi-Objective Optimization of aluminum hollow tubes for vehicle crash energy absorption using a genetic algorithm and neural networks. *Thin-Walled Structures, 49*(12), 1605-1615. doi:10.1016/j.tws.2011.08.009

Mirzaei, M., Shakeri, M., Sadighi, M., & Seyedi, S. (2011). Multi-objective optimization of crashworthiness of cylindrical tubes as energy absorbers. *Iranian Journal of Mechanical Engineering (English), 12*(1), 5-18.

Niknejad, A., Abedi, M. M., Liaghat, G. H., & Zamani Nejad, M. (2012). Prediction of the mean folding force during the axial compression in foam-filled grooved tubes by theoretical analysis. *Materials & Design, 37*, 144-151. doi:10.1016/j.matdes.2011.12.032

Reid, S., Reddy, T., & Gray, M. (1986). Static and dynamic axial crushing of foam-filled sheet metal tubes. *International Journal of Mechanical Sciences, 28*(5), 295-322.

Rezvani, M., Nouri, M. D., & Rahmani, H. (2012). Experimental and numerical investigation of grooves shape on the energy absorption of 6061–T6 aluminium tubes under axial compression. *International Journal of Materials and Structural Integrity, 6*(2), 151-168.

Rezvani, M. J., & Nouri, M. D. (2013). Axial Crumpling of Aluminum Frusta Tubes with Induced Axisymmetric Folding Patterns. *Arabian Journal for Science and Engineering, 39*(3), 2179-2190. doi:10.1007/s13369-013-0734-7

Rezvani, M. J., Nouri, M. D., & Rahmani, H. (2012). Experimental and numerical investigation of grooves shape on the energy absorption of 6061-T6 aluminium tubes under axial compression. *International Journal of Materials and Structural Integrity, 6*(2), 151-168.

Salehghaffari, S., Rais-Rohani, M., & Najafi, A. (2011). Analysis and optimization of externally stiffened crush tubes. *Thin-Walled Structures, 49*(3), 397-408.

Seitzberger, M., Rammerstorfer, F. G., Gradinger, R., Degischer, H., Blaimschein, M., & Walch, C. (2000). Experimental studies on the quasi-static axial crushing of steel columns filled with aluminium foam. *International Journal of Solids and Structures, 37*(30), 4125-4147.

Shakeri, M., Mirzaeifar, R., & Salehghaffari, S. (2007). New insights into the collapsing of cylindrical thin-walled tubes under axial impact load. *Proceedings of the Institution of Mechanical Engineers, Part C: Journal of Mechanical Engineering Science, 221*(8), 869-885.

Thornton, P. (1980). *Energy absorption by foam filled structures* (0148-7191). Retrieved from

Vaughn, N. A. (2007). Design-Expert® software. *Stat-Ease, Inc, Minneapolis, MN*.

Yamada, Y., Banno, T., Xie, Z., & Wen, C. (2005). Energy absorption and crushing behaviour of foam-filled aluminium tubes. *Materials transactions, 46*(12), 2633.

Zarei, H. R., & Kröger, M. (2006). Multiobjective crashworthiness optimization of circular aluminum tubes. *Thin-Walled Structures, 44*(3), 301-308. doi:10.1016/j.tws.2006.03.010

Nomenclature

$E_{absorbed}$	Absorbed energy
P_m	Mean crushing load
P_{max}	Maximum crushing load
CFE	Crushing force efficiency
SEA	Specific energy absorption
ρ	Foam density
D_i	Inner diameter of tube
λ	Groove distances
N	Number of grooves
t	Thickness of tube
d	Groove depth
$t' = t - d$	Wall thickness in groove
L	Tube length
σ	Engineering stress
ε	Engineering strain
E	Young's modulus
σ_{yield}	Yield stress
ε_D	Densification strain
m_{tube}	Tube mass

This article can be cited: Shahravi S. Rezvani M.J. & Jahan A. (2019). Multi-response Optimization of Grooved Circular Tubes Filled with Polyurethane Foam as Energy Absorber . *Journal of Optimization in Industrial Engineering*. 12 (1), 133- 149.

http://www.qjie.ir/article_543688.html
DOI: 10.22094/JOIE.2018.764.1487